

From structural diversity measures to ecosystem complexity: Experiments for deriving aggregated complexity indices

Sebas de Smedt , Norul Sobuj , Arne Pommerening ^{*}

Swedish University of Agricultural Sciences SLU, Faculty of Forest Sciences, Department of Forest Ecology and Management, Skogsmarksgränd 17, SE-901 83 Umeå, Sweden



ARTICLE INFO

Keywords:

Location diversity
Size diversity
Species diversity
Plant diversity indices
Arithmetic-geometric aggregation
Random weights
Continuous cover forestry (CCF)

ABSTRACT

In times where biodiversity is globally under much pressure, effective monitoring of ecosystems is of great importance. As plants and particularly trees tend to shape the physical environment of ecosystems, indicators based on the structural complexity of plant communities are frequently used as surrogates for direct measures of biodiversity. A multitude of such quantitative diversity indicators exist and when considering multiple ecosystem services there is often the need to aggregate them in a single complexity index. We quantified the effects of four statistical techniques of aggregating contributing indices from three overarching tenets of α -diversity, i.e. location (or dispersion) diversity, size and species diversity. In addition we experimentally studied the influence of four different weights assigned to the contributing diversity measures. Overall the differences between the weights and aggregation methods used were comparatively small. Inverse correlation weights combined with arithmetic-geometric aggregation turned out to be the best choice for obtaining a clear complexity gradient for our study data from the boreal forest in Northern Sweden. In our analysis, it proved useful to rely on a small pool of global reference data with a strong structural gradient which served as contrasts and training data in addition to the data of our study plots. The application of random weights as statistical references was very helpful for understanding how weighting and index aggregation works. Our index-aggregation results suggested that the nine Swedish forest plots were at the lower end of global complexity and differed comparatively little in terms of forest structure.

1. Introduction

It is now well established that diversity in ecosystems is not an unnecessary ‘luxury’ property but fundamental to their existence (Yachi and Loreau, 1999; Begon et al., 2006; Matias et al., 2013; Oliver et al., 2015; Danet et al., 2024). Ulrich et al. (2023) stated that biodiversity also benefits human well-being and particularly human health. Therefore biodiversity is not only an essential notion of ecosystems but also an ecosystem good or commodity (Sandifer et al., 2015). Currently biodiversity is threatened by multiple man-made global changes, among which climate change potentially has a particularly detrimental effect (McElwee, 2021; Román-Palacios and Wiens, 2020). Worldwide conservation is therefore concerned with maintaining diversity or at least with slowing down the process of losing species (Carvalheiro et al., 2013). Key to effective conservation is goal-oriented monitoring including the application of specialised summary statistics for measuring the current state of plant diversity and their aggregation in

complexity indices (Weiner and Solbrig, 1984; Pommerening and Grabinik, 2019).

Biodiversity can be quantified in multiple ways by focussing on a wide range of different taxa involving plants, fungi and animals. As plants play an important role in shaping the physical structure of many environments, the structural complexity of plant communities has frequently been used as an indicator of the diversity in other taxa (Recher et al., 1996; Moen and Gutierrez, 1997; Beckschäfer et al., 2013). The *habitat heterogeneity hypothesis* (Simpson, 1949; MacArthur and Wilson, 1967) relates the positive association between species diversity and structural complexity by suggesting that more complex environments provide increased niche space and thus facilitate specialisation and avoidance of competition through spatial segregation (Cramer and Willig, 2005; Beckschäfer et al., 2013). When considering plant ecosystems, α -diversity or functional diversity at community level is often subdivided into various tenets or facets. Carmona et al. (2016) and Wojcik et al. (2025), for example, focussed on functional diversity

* Corresponding author.

E-mail address: arne.pommerening@slu.se (A. Pommerening).

and therefore considered the tenets of functional richness, functional evenness and functional divergence, which, in their view, together defines the trait space used by an ecosystem. In this study, we alternatively considered structural diversity and its tenets *location* (or *dispersion*) diversity, *size* diversity and *species* diversity (Gadow, 1999; Pommerening, 2002; cf. Fig. 1). The diversity of plant locations reflects the pattern of plant dispersion, e.g. regular, clumped (clustered), random locations or some combination of these. Species diversity is concerned with species richness, species abundance and the spatial arrangement of species. Size diversity involves the distribution and spatial arrangement of, for example, tree stem diameters or heights. Size diversity is particularly important in ecosystems that involve plants such as trees whose sizes are extremely variable. Size-diversity measures can be further subdivided into indices of size inequality and size dominance.

Size inequality measures focus on size variability in plant populations, whilst size dominance measures attempt to address matters of competition.

There is consensus that all three tenets location (or dispersion) diversity, size diversity and species diversity jointly contribute to overall structural complexity (Pommerening and Stoyan, 2008; Bäuerle and Nothdurft, 2011; Wudel et al., 2023). In monitoring and diversity analyses, it is possible to consider the results relating to the three diversity tenets and even the results of individual diversity indices independently. However, there is often a need to synthesise all index results into a single number to establish overall complexity (Jaehne and Dohrenbusch, 1997; Wojcik et al., 2025). There are many definitions of complexity, however, the most intuitive describes the level of biological integration and interaction in ecosystems. The term ecosystem itself focuses on the structure, the complexity of organisation and the functioning of the system (Kimmens, 2004). In this study, we mainly focused on structural complexity (Ehbrecht et al., 2017, 2021) as created by the dominant life forms of an ecosystem, e.g. the trees of a forest ecosystem. Complexity is a valuable ecosystem trait that directly relates to ecological resilience (Messier et al., 2013). This is typically the case when diversity trends over temporal or spatial gradients are examined. Aggregating single diversity indices in a comprehensive measure is not trivial and carefully examining different methods is often not taken seriously into consideration. The general statistical process of constructing complexity measures by aggregation is outlined in Fig. 2, which also indicates the corresponding sections of this article. In this process, there are several methodological questions involving which diversity measures to choose and others relating to the aggregation of indices.

The objective of this study was to identify the most appropriate way to derive global structural complexity from individual diversity indices. For this we examined different multivariate weighting and aggregation techniques and their relative influence on the results. To our knowledge, in all previous studies aggregation methods were deterministically selected without carrying out sensitivity analyses of alternative

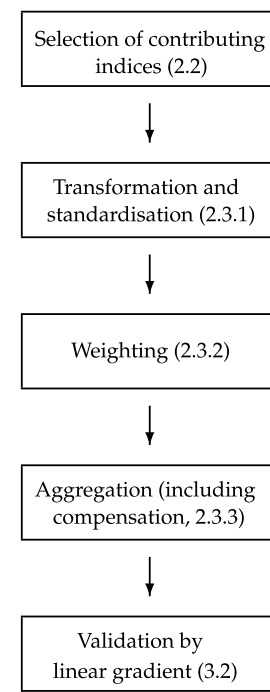


Fig. 2. Flow chart for deriving aggregated complexity indices from individual diversity measures. The numbers in brackets give the respective sections in this article.

approaches. In many different ecological contexts, deriving global structural complexity is necessary, for example, when assessing biodiversity as one ecosystem commodity among many others (Ehbrecht et al., 2017, 2021; Wojcik et al., 2025; Zhao et al., 2022). Nine plots from the boreal forest of Northern Sweden were used for that purpose and additionally complemented by well-known contrast or reference forest plots from different parts of the world for establishing a meaningful global diversity gradient and for ensuring the robustness of both the methodology and the resulting complexity index. We first applied the unique complexity index to the eight reference plots and then used the nine plots from Sweden for quantifying their complexity in the global context of the reference data. This resulted in a total of 17 forest plots and another objective was to identify the position of the nine Swedish plots in this global complexity gradient.

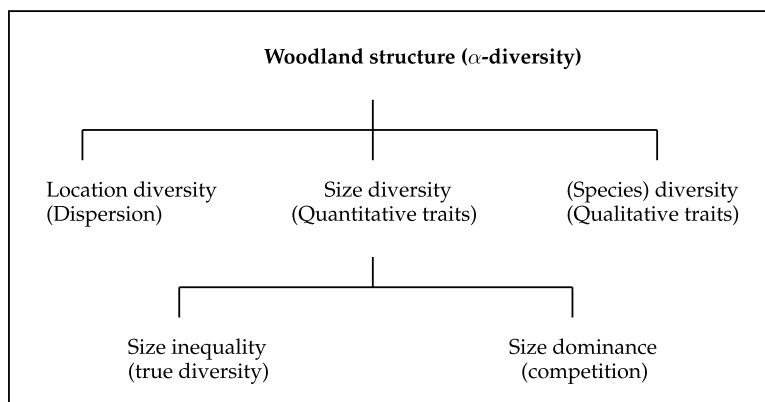


Fig. 1. The three major tenets of structural diversity. Modified from Pommerening (2002).

2. Materials and methods

2.1. Study data

The main focus of this study is on the Svarthberget data (Section 2.1.1) and contrast or reference data (Section 2.1.2) were added to ensure that the complexity scale was not biased by the use of only local data and that the final complexity index is universally applicable. Selecting eight plots appeared to be reasonable in an attempt to approximately match the number of the Svarthberget plots. These eight plots were selected for their relative differences and merits in other studies which we referred to in Section 2.1.2. The contrast data were described in the order of complexity as can be inferred from Table 1. Unique identification (ID) ranks were assigned to them in the same order and used in the analysis.

2.1.1. Svarthberget data (ID ranks 1–9)

Near the SLU Svarthberget field station close to Vindeln in Northern Sweden three sites were selected in the boreal forest with a structural gradient ranging from simple to medium and complex forest structure, which was assigned as part of project fieldwork based on the visual appearance of vertical forest structure. Simple forest structure was defined as a combination of mature overstorey and a comparatively low understorey layer stemming from a single regeneration cohort. According to our definitions, medium structure includes an additional older regeneration cohort whilst complex forest structure has at least three canopy layers. One of the objectives of this project was to verify the visual assignment of plots to the aforementioned complexity classes simple, medium and complex. We established three plot replicates with an average size of 50 × 50 m in each of these three sites at approximately 230 m asl. The main species were Norway spruce (*Picea abies* L.) and Scots pine (*Pinus sylvestris* L.). They were complemented by broadleaved species, mainly birch (*Betula* spp.), willow (*Salix* spp.), aspen (*Populus tremula* L.), and grey alder (*Alnus incana* L.). The dominating soil type is moraine of varying thickness.

2.1.2. Contrast/reference data

Clocaenog Forest (Wales, UK) lies on the southern side of the Densbig moors, a plateau rising to between 300 m and 500 m asl. The forest stands (Tyfiant Coed plots 1 and 2 at 53.07 N, 3.43 W, ID ranks 10 and 11) included in this study are situated at an altitude of 395 m asl. Intergrade iron pan soil predominates on this site. The site was originally planted with Sitka spruce (*Picea sitchensis* (BONG.) CARR. and lodgepole pine (*Pinus contorta* DOUGL. ex LOUD.) in 1951. *P. sitchensis* now dominates the site and plot 2 is structurally slightly more diverse in terms of tree dispersion and vertical tree height structure than plot 1 (Pommerening et al., 2024).

The Białowieża data (ID rank 12) are from Białowieża Forest (50.43 N, 23.50 E) in eastern Poland in the border zone between Poland and Belarusia. This diverse woodland consists of a pedunculate oak

(*Quercus robur* L.) overstorey interspersed with Scots pine (*Pinus sylvestris* L.) and an understorey of Norway spruce (*Picea abies* (L.) KARST.), hornbeam (*Carpinus betulus* L.) and silver birch (*Betula pendula* Roth.). The data are from outside the strict reserve of Białowieża Forest and the forest stand is managed for biodiversity and timber value according to the principles of low-impact continuous cover forestry (Pommerening and Stoyan, 2008; Pommerening and Uria-Diez, 2017).

The Hidegvizvölgy woodland (ID rank 13) is located in the buffer zone of the Hidegvizvölgy Forest Reserve (47.34 N, 17.37 E) in the hills around the northwest Hungarian city of Sopron. Before being designated as a forest reserve in the early 2000s, the area was part of the restricted border zone of the Iron Curtain for almost 50 years and consequently remained undisturbed for a comparatively long time (Puttkamer, 2005; Pommerening and Uria-Diez, 2017). The main species of this forest stand include sessile oak (*Quercus petraea* MATT.), hornbeam (*Carpinus betulus* L.) and European beech (*Fagus sylvatica* L.).

Deisenhofener Forst (ID rank 14) is a monitoring plot near Munich (Germany, 47.96 N, 11.70 E) located in a forest which is in advanced transition to continuous cover forestry (Pommerening, 2023). The forest stand is located in the Munich gravel plain which formed during late Pleistocene glacial periods. The plot involves several canopy layers. Dominant species are Norway spruce (*Picea abies* (L.) KARST.) and silver fir (*Abies alba* MILL.) with strong contributions of European beech (*Fagus sylvatica* L.) and Scots pine (*Pinus sylvestris* L.). Minor species include *Abies grandis* (DOUGL.) LINDL., *Quercus rubra* L., *Carpinus betulus* L. among others which partly resulted from natural regeneration and partly from underplanting (Füldner, 1995).

Freyung (ID rank 15) represents a diverse selection forest located in the Bavarian Forest (51.68 N, 10.10 E, Germany) not far from the border between Germany and the Czech Republic. The forest plot has several canopy strata and the main species are Norway spruce (*Picea abies* (L.) KARST.), silver fir (*Abies alba* MILL.) and European beech (*Fagus sylvatica* L.). Situated at 720 m asl with south-eastern exposition the main soil type is a podsolised stony brown earth. The management principles of Freyung involved single-tree removals and a continuous long-term regeneration (Pommerening et al., 2000).

Xiaolongshan Forest (ID rank 16) is located in the Xiaolongshan Nature Reserve, Gansu province, north-west China. The forest is situated on the north-facing slopes of the West Qinling Mountain range (33.30–34.49 N, 104.22–106.43 E) and constitutes a natural mixed pine-oak forest. The soil type is a grey cinnamon soil in the north of the Qinling Mountains and yellow cinnamon soil prevails in the south. Plot b from the Xiaolongshan Forest was included in this study. This stand is a mixed pine-oak population dominated by *Quercus aliena* var. *acuteserrata* MAXIM., *Ulmus glabra* Huds. and *Symplocos paniculata* (THUNB.) WALL ex D. DON. (H. Wang et al., 2021).

Tazigou Experimental Forest Farm (43°05'–43°40' N, 129°56'–131°04' E) is located in Jilin Province, China (H. Wang et al., 2021) and has ID rank 17. This area of secondary forest is situated on

Table 1

Main characteristics of 17 experimental woodland data sets: Area in hectare, *A*, global species richness, i.e. the absolute number of species, *S*, number of trees per hectare, *N*, basal area, *G*, minimum stem diameter, *d_{min}*, maximum stem diameter, *d_{max}*, quadratic mean stem diameter, *d_g*, height of the largest 100 trees per hectare, *h₁₀₀*. The three replicates of the Svarthberget sites (simple, medium and complex structure) were summarised jointly.

Characteristic	<i>A</i> [ha]	<i>S</i>	<i>N</i> [ha ⁻¹]	<i>G</i> [m ² ha ⁻¹]	<i>d_{min}</i> [cm]	<i>d_{max}</i> [cm]	<i>d_g</i> [cm]	<i>h₁₀₀</i> [m]
Svarthberget (s)	0.26	4	1237.03	27.90	4.0	33.1	16.9	33.04
Svarthberget (m)	0.22	4	745.43	11.88	4.0	43.3	13.1	18.93
Svarthberget (c)	0.22	3	1222.32	12.48	4.0	35.5	13.7	16.43
Clocaenog 1	1.00	1	291.88	30.30	20.4	55.5	36.4	28.69
Clocaenog 2	1.00	4	330.03	29.85	4.2	59.2	33.9	27.43
Białowieża	1.02	5	748.95	34.92	5.0	79.1	24.4	32.79
Hidegvizvölgy	0.67	7	782.09	24.43	6.2	57.2	26.9	24.68
Deisenhofen	1.13	11	1106.49	45.63	6.5	80.6	22.9	32.94
Freyung	0.50	3	458.75	41.98	6.8	92.1	34.1	36.22
Xialongshan	0.49	35	841.66	25.31	4.4	70.5	19.6	18.98
Tazigou	1.00	13	1202.00	20.19	4.0	55.7	14.6	17.31

Laoyeling Mountain of the Changbai Mountain range. The area has predominantly dark brown soil (humic cambisols) with a high natural fertility. The main tree species are Mongolian oak (*Quercus mongolica* Fisch. ex Lebed.), Asian white birch (*Betula platyphylla* Sukaczew), Korean pine (*Pinus koraiensis* Siebold & Zucc.), Ussuri popular (*Populus ussuriensis* Komarov) and Amur lime (*Tilia amurensis* Rupr.). The mapped forest stand included in this research is plot c in Tazigou.

The tree density, size and species characteristics reveal that the nine Svatberget plots fit well into the variety of different values of these characteristics given by the eight contrast plots (Table 1). The Svatberget plots have more trees than most contrast plots, but are exceptionally low in basal area on the medium and complex structure site. The same applies to the quadratic mean diameter. The mean of the 100 dominant trees per hectare is also much lower at Svatberget than in most of the contrast plots.

2.2. Individual, contributing diversity indices

The selection of individual diversity indices was carried out so that index representatives of all three diversity tenets, i.e. location, species and size diversity were included. Dominance indices were deliberately excluded, since they are primarily not intended to quantify size diversity but competition. Based on a literature review, we selected contributing structural indices that had performed well in the past and whose indicative power is well documented.

2.2.1. Dispersion (plant location diversity)

2.2.1.1. Horizontal structure. Spatial distribution patterns profoundly influence plant growth, habitats and regeneration (Pretzsch, 1995). For characterising plant dispersion, *aggregation index R'* by Clark and Evans (1954) compares the mean of observed distances \bar{r} between any plant of a spatial plant pattern with the corresponding mean distance Er of a theoretical pattern with complete spatial randomness:

$$R' = \frac{\bar{r}}{Er} \text{ where } Er = 0.5 \times \sqrt{\frac{N}{A}} \quad (1)$$

In Eq. (1), A is the plot area and N is the total number of trees. The aggregation index has proved to be a very efficient index of plant location diversity (Corral-Rivas, 2006).

2.2.1.2. Vertical structure. Vertical structure of plant ecosystems is likely to have an even greater influence on overall complexity than horizontal structure. According to Falster and Westoby (2003), vertical structure is one of the most important notions of ecosystems involving trees, since raising their foliage into considerable heights above ground is the main evolutionary strategy of these plant types. Zenner and Hibbs (2000) defined the *structural complexity index* (SCI), which synthesises vertical structure by means of Delaunay triangulations where tree locations provide x and y coordinates and total tree height serves as z coordinate. By a spatial tessellation approach (Delaunay, 1934) each tree is connected to its neighbours such that triangles are defined that form a continuous faceted surface, i.e. a *triangulated irregular network* (TIN; Beckschäfer et al., 2013). SCI is defined as the ratio of the total surface area of this TIN and the projected ground area of the constituent triangles:

$$V = \frac{\text{Surface area of TIN}}{\text{Projected area of TIN}} \quad (2)$$

The ratio given in Eq. (2) tells us how much forest structure varies vertically compared to a flat surface made up of individual triangles (Zenner and Hibbs, 2000; Beckschäfer et al., 2013) and essentially quantifies *canopy roughness* or *rugosity*. As such SCI is related to photosynthesis and resilience. If all trees have the same total height, V equals 1, which is the lower limit of this index. For structurally more complex

forests, $V > 1$. An edge correction method excludes border triangles that are affected by spatial edge effects.

2.2.2. Species diversity

2.2.2.1. Species richness and spatial species mingling. Spatial *species mingling* describes the spatial interaction of plant species, i.e. how individual plants of certain species are spatially mixed with those of other species (Pommerening et al., 2024). The mingling index is defined as the proportion of heterospecific pairs successively formed by a given plant i and its k nearest neighbours (Gadow, 1993; Eq. (3)). In the analysis, every plant within a given research or sample plot acts once as plant i (also referred to as *reference* or *subject plant*):

$$M_i = \frac{1}{k} \sum_{j=1}^k \mathbf{1}(m_i \neq m_j) \quad (3)$$

Function $\mathbf{1}(A)$ is an indicator function with $\mathbf{1}(A) = 1$, if A is true, otherwise $\mathbf{1}(A) = 0$. The population mingling index computed for the entire plant community in a given plot is calculated as the arithmetic mean of all M_i by considering an appropriate edge correction. We applied the NN1 edge correction method (Pommerening and Stoyan, 2006). The species mingling index complements species richness by spatial information. However, Pommerening and Särkkä (2025) demonstrated that the concept of spatial species mingling partially also includes local species richness, i.e. species richness in the neighbourhood of reference plant i .

When constructing our complexity index, we applied the species mingling index to Voronoi neighbourhoods. Voronoi neighbours tend to better describe interactions from an individual-plant perspective, since the neighbourhood covers 360° around the reference plant. This property makes Voronoi neighbours more interesting for ecological studies (Pommerening et al., 2024).

2.2.2.2. Vertical species diversity. The fundamental idea of the *species profile index* used in this study is to quantify species diversity in different vertical layers or height bands. This concept is also partly motivated by the fact that vertical forest structure is of great importance when quantifying overall forest diversity. The index gives an idea of the vertical extent of species diversity and to some degree also of vertical niche partitioning across canopy layers (Pretzsch 1995). Based on the original species profile index by Pretzsch (1995), we modified his concept to consider $c = 4$ height bands and the Simpson (1949) species diversity index. In this study, species profile index A' is the complement of the sum of the Simpson index calculated separately for c relative height bands:

$$A' = \sum_{i=1}^S \mathbf{1} - \sum_{j=1}^c p_{ij}^2 \quad (4)$$

In Eq. (4), S is the number of species (global species richness), c is the number of height bands, i.e. $c = 4$ in this case, and p_{ij} is the proportion of species i in band j . The four height bands are defined by 25 %, 50 %, 75 % and 100 % tree total height percentiles. The trees of each plot are assigned to one of the four height bands [0, 25 %), [25 %, 50 %), [50 %, 75 %) and [75 %, 100 %) depending on the vertical locations of their crown tips. Species profile index A' is higher in plots with more vertical height differentiation compared to a single-canopy forest stand (Pommerening, 2023).

2.2.3. Size diversity

2.2.3.1. Spatial stem diameter differentiation. Size differentiation index T_i focuses on the size contrast between a reference plant and its nearest Euclidean neighbour. For each plant i and its first nearest neighbour k , T_i is defined as the ratio of smaller-sized and larger-sized variables of subject plant and first nearest neighbour subtracted from one (Gadow,

1993):

$$T_i = 1 - \min \left(\frac{m_i}{m_k}, \frac{m_k}{m_i} \right) \quad (5)$$

In Eq. (5), m_i and m_j are the size variables of the subject plant and its first neighbour, respectively. In the construction of the complexity index, diameter at breast height (dbh) was used as tree size variable when calculating Eq. (5). In forest ecosystems, size differences between trees and their first Euclidean neighbours are often larger than between trees and subsequent Euclidean neighbours (e.g. 2nd, 3rd or 4th nearest neighbours) and give a meaningful description of overall spatial size variability.

2.2.3.2. Overall non-spatial size diversity. The Gini coefficient (G') is a well-established measure of inequality adapted from economics (Gini 1912; Lorenz 1905) for quantifying size diversity. It has proved to capture the non-spatial size structure of forest stands well (Damgaard and Weiner, 2000; Duduman, 2011). Using individual-tree basal area g_i , sorted in ascending order, the equation used in this study is:

$$G' = \frac{2 \sum_{i=1}^n g_i \times i}{n \sum_{i=1}^n g_i} - \frac{n+1}{n} \quad (6)$$

The Gini coefficient is calculated to account for possible bias in finite samples in a standardised manner (Eq. (7)).

$$G^* = G' \times \frac{n}{n-1} \quad (7)$$

The sample size adjustment ensures unbiasedness in smaller plots with few trees (Pommerening et al. 2016; Pommerening 2023). The larger the Gini coefficient the more diverse the size structure of a plant ecosystem.

2.2.4. Density and disturbance

Additionally to the three aforementioned tenets of plant diversity and six diversity indices, plant density is often considered and important structural characteristic (Pretzsch, 2009; Beckschäfer et al., 2013). The slenderness or height-diameter ratio of trees is strongly influenced by tree density. Disturbances – whether natural or human – typically reduce tree density and encourage trees to grow relatively more in stem diameter than in total height, which in the long term results in lower height-diameter ratios than before the density reduction (Pretzsch, 2009; Wenk et al., 1990; Pommerening and Grabarnik, 2019). Slenderness is therefore an indirect indicator of density with a legacy effect, since it takes some time for height-diameter ratios to adjust to changing environmental conditions. As a contributing index we decided to focus on the tree overstorey and thus we calculated the mean of the 20 %-tallest trees per plot:

$$\bar{s} = \frac{1}{n} \sum_{i=1}^n \frac{h_i}{d_i} \text{ for } h_i > 0.8 \times h_{\max} \quad (8)$$

h_i and d_i represent tree total height and stem diameter. \bar{s} is usually smaller than 1. Density and tree morphology characteristics are first-order measures of forest structure and therefore also indicate structural diversity.

2.3. Complexity index construction

When constructing a global complexity index, the aggregation of contributing individual indices includes (1) transformation and standardisation, (2) weighting of constituent diversity indices and (3) the actual aggregation method by which the final, overall complexity index is calculated from the individual indices (Fig. 2; Mazziotta and Pareto, 2013; Beliakov et al., 2015).

2.3.1. Transformation and standardisation

Standardisation aims to make the component diversity indices operate at the same scale. A common way to ensure this is by requiring the indices to lie between 0 and 1. For species mingling (Eq. (3)), stem-diameter differentiation (Eq. (5)) and the Gini index (Eq. (7)) standardisations of this kind were not necessary, as these indices by definition only take values between 0 and 1. For the remaining diversity indices suitable standardisations were identified. In some cases, first transformations were necessary so that large standardised index values imply high diversity and low index values indicate low diversity. For example, in the case of the aggregation index (Eq. (1)), R' was subtracted from maximum value 2.1451, as small values of original R' indicate clustering or inhomogeneity, which implies high diversity in this case. A similar transformation had to be applied to the structural complexity index (Eq. (2)) and for the slenderness of dominant trees (Eq. (8)). Details are given in Table 2.

2.3.2. Weighting

Weights offer information about the relative importance of individual component indices and their sum usually equals 1. They can be chosen according to expert judgement. Although this strategy of assigning weights seems plausible and is justifiable, it may appear to be somewhat subjective and therefore of limited value.

An alternative, more objective weighting approach is to base the component indices on quantitative criteria. Two obvious options are random and uniform weights. As often applied in statistics, *random weights* can serve as a reference to compare the results from other weights with and can be computed by drawing uniform random numbers between 0 and 1 for each contributing index. The results are then divided by the sum of these random numbers to ensure that the weights sum to 1. We repeated the allocation of random weights 1000 times and calculated mean weights and standard deviations from the 1000 results. *Uniform weights* are computed as the reciprocal of the number of contributing indices. This reciprocal (in our case 0.143, cf. Table 2) is then the same weight for all indices.

Another strategy for the choice of weights is to balance index representation by considering the correlation structure of the contributing indices. For example, those indices that have a lower absolute correlation with other indices are given a larger weight and vice versa. This weighting can be achieved by basing the weights on the inverse of the mean absolute Pearson correlation coefficients of each component index

Table 2

Contributing diversity indices, their standardisation and four of the five index weights used in the aggregation process. Standardisation often also includes transformation. Clark and Evans (1954) aggregation index, R' (Eq. (1)), structural complexity index (SCI), V (Eq. (2)), mean spatial species mingling, \bar{M} (Eq. (3)), species profile index, A' (Eq. (4)), mean stem-diameter differentiation, \bar{T} (Eq. (5)), Gini coefficient, G' (Eq. (7)), and mean height-diameter ratio of dominant trees, \bar{s} (Eq. (8)). Corr. – inverse correlation, PCA – principal component analysis.

Diversity index	Standardisation	Uniform weights	Corr. weights	PCA weights
R'	$\frac{x - \min(x)}{2.1451 - \min(x)}$ with $x = 2.1451 - R'$	0.143	0.104	0.162
V	$1 - \frac{1}{V}$	0.143	0.134	0.160
\bar{M}	-	0.143	0.127	0.162
A'	$\frac{A'}{c}$	0.143	0.112	0.162
\bar{T}	-	0.143	0.170	0.127
G'	-	0.143	0.112	0.169
\bar{s}	$\begin{cases} 1 - \bar{s} & \text{for } \bar{s} < 1 \\ 0 & \text{otherwise} \end{cases}$	0.143	0.242	0.043

so that the weights' total sum again equals 1 as previously mentioned. This *inverse-correlation method* reduces the influence of redundant information and assigns higher weights to indices that potentially contribute unique insight and novelty to the aggregated complexity index (Mazziazzo and Pareto, 2013).

An alternative way of deriving weights is to use *principal component analysis* (PCA; Legendre and Legendre, 2012). The loadings of the first principal component accounts for the largest variance in the original data and may also serve as objective weights (Wold et al. 1987; Chao and Wu, 2017). These loadings can be transformed to weights by limiting their sum to 1. PCA tends to assign the highest weights to those diversity indices that have the highest mean absolute correlation with other indices.

The Pearson correlation coefficient between inverse-correlation and PCA weights is -0.99 , thus highlighting that both weighting methods pursue quite opposite strategies. A disadvantage of inverse-correlation and PCA methods is that they depend on the tree data including possible contrast/training data used for constructing the aggregated complexity index and the calculated weights may differ from those that apply to other data.

We applied all of the objective weighting methods described in this section in our experiments.

2.3.3. Index aggregation

The last step in constructing a complexity index is the actual aggregation of individual component indices. We assumed that at least to some degree large values of some component indices can compensate for small values of others, e.g. a lack of species diversity can to some extent be compensated for by more size diversity. Classic aggregation methods include the mathematical operations of summation and multiplication. In all following aggregation approaches, weights are generally assumed to be non-negative and to sum to 1.

In the process of summation, all component weights are summed up whilst being multiplied by the corresponding weights to result in a *weighted arithmetic mean*:

$$C^{(a)} = \sum_{i=1}^n w_i x_i \quad (9)$$

Here x_i are standardised component indices and w_i are the corresponding weights. The number of component indices is denoted by n . Weighted arithmetic means such as $C^{(a)}$ have perfect compensatory properties.

When aggregating indices in a multiplicative way, each transformed and standardised index x_i is raised to the power of its weight w_i and multiplied by other transformed and standardised component indices:

$$C^{(g)} = \prod_{i=1}^n x_i^{w_i} \quad (10)$$

The result is *weighted geometric mean* $C^{(g)}$. In general, weighted geometric means are less compensatory than arithmetic means.

Finally, a third type of diversity index aggregation can be derived from *weighted harmonic means*, which is the mean of the index reciprocals:

$$C^{(h)} = \sum_{i=1}^n \frac{w_i}{\frac{1}{x_i}} \quad (11)$$

The weighted harmonic mean is the least compensatory of the three aggregation methods and is often applied to rates and ratios. Eqs. (9), (10) and (11) ensure that the aggregated complexity index lies between 0 and 1 just like the component indices.

We also considered combined *arithmetic-geometric aggregation* by calculating the arithmetic mean of $C^{(a)}$ (Eq. (9)) and $C^{(g)}$ (Eq. (10)), which we notationally referred to as $C^{(ag)}$.

Traditionally in multivariate analysis, radar plots have often been used to compare the diversity in different ecosystems by visually considering the areas created by the radar charts. Theoretically this area can be quantified, however, the result is strongly influenced by the order in which the component diversity indices are displayed (ElMaraghy et al., 2014). This is a clear deficit of radar plots despite their visual appeal. For their traditional importance we used radar plots in this study as descriptive statistics.

We organised complexity indices C in bar charts so that each bar represented one of the 17 plots and ordered the bars according to C in a descending order. For best allocation of complexity indices and ranks we were interested in obtaining gradients of C as smooth and linear as possible. When comparing many forest ecosystems across subtropical, temperate and boreal climate zones as in our study, a linear gradient implying a constant rate of decrease in complexity is beneficial because this allows to see differences in structural complexity more clearly. As a validation characteristic (cf. Fig. 2), we measured how far each sequence of ordered C or bars was removed from the linear gradient by linear-gradient measure \tilde{c} , which is the ratio of squared median of q divided by the standard deviation of q . Here, $q = \frac{C_i}{C_{i+1}}$ is the ratio of two successive values of C after arranging them in descending order. Values of q usually lie between 1 and 2, $q > 2$ can be considered as outliers. \tilde{c} is a variant of the coefficient of variation where we used the median instead of the mean to avoid outliers (leading to sharp drops in the C sequence).

3. Results

3.1. First complexity impression using simple radar charts

Radar charts using the unweighted index values give a first impression of the overall complexity of the 17 woodland data. When depicting the seven diversity indices a polygon area is created which seems to suggest that it can serve as a measure of overall complexity and areas can potentially be compared between woodlands.

As explained in Section 2.3.3, caution needs to be applied when interpreting radar charts (ElMaraghy, 2014). Nevertheless, for their traditional popularity the radar charts presented in Fig. 3 may serve as convenient descriptive statistics to introduce our results.

We can clearly see that there is a complexity trend in the contrast data where the polygon area is mostly and gradually increasing from Clocaenog (plot 1) to Tazigou. This effect was, of course, intended when assembling the contrast data. The gradual differences between plots sometimes appear to be difficult to appreciate, as not all characteristics increase from plot to plot (cf. Fig. 3). This is, of course, natural and as discussed in Section 2.3.3 the idea of complexity indices is that some contributing individual diversity indices can to a certain degree compensate for others. Considering the anticipated diversity trend, the Svarberget plot data appear to fit somewhere between Clocaenog (plot 3) and Bialowieża. Within the nine Svarberget plots we can conclude that the first three plots show low overall diversity, although indices V and \bar{T} tend to have comparatively high values. The differences in terms of polygon areas between Svarberget plots 4–9 are quite small and it seems difficult to identify a clear trend from the radar charts (Fig. 3).

3.2. Different weights and aggregation methods

When comparing the bar charts in Fig. 4 it is evident that the results in terms of complexity index C are quite similar in all 16 charts

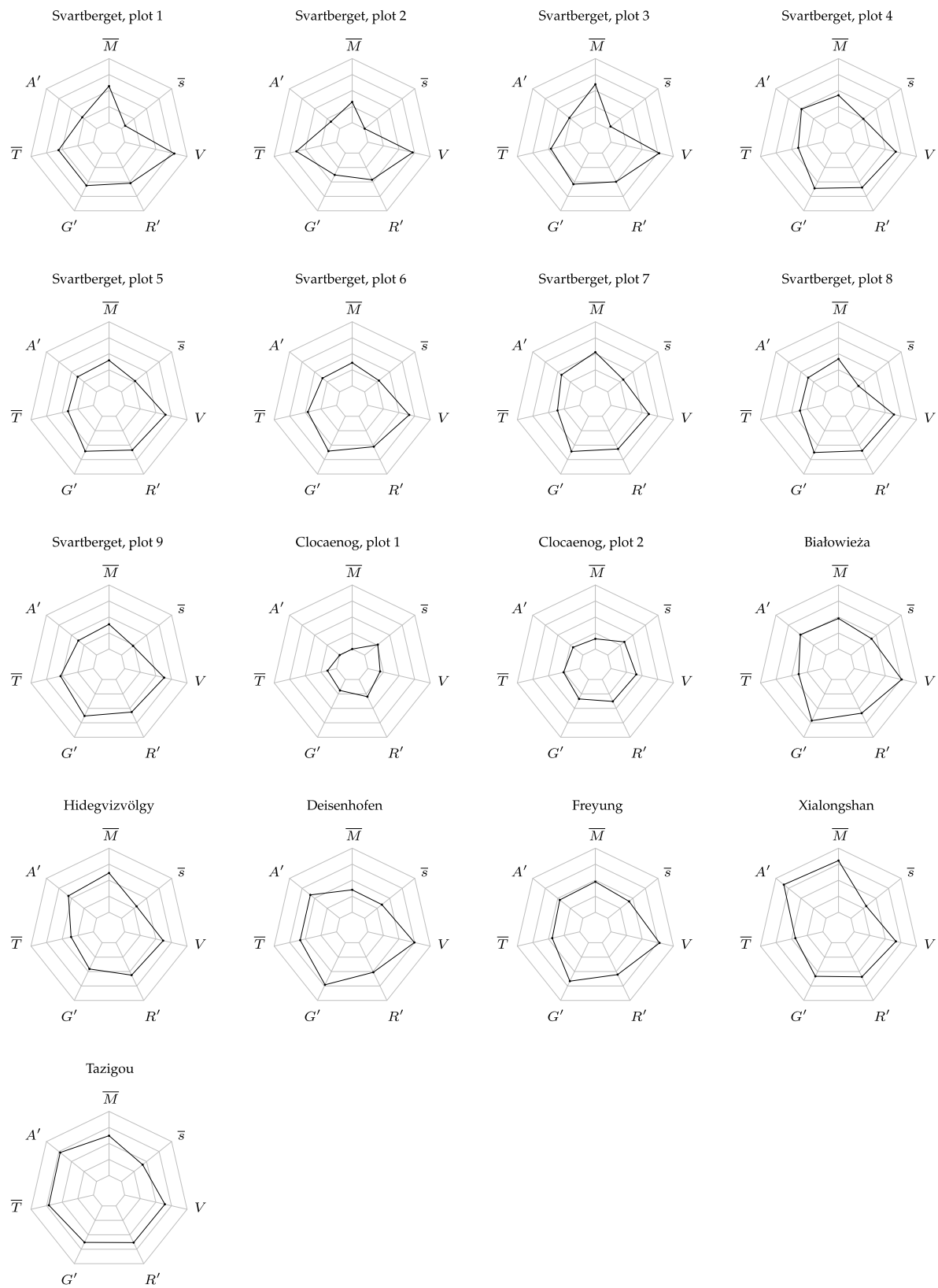


Fig. 3. Radar charts based on the `fmsb` R package depicting the unweighted values of the seven diversity indices selected in this study for characterising α -diversity of 17 study plots after transformation and standardisation. The contributing indices considered are Clark and Evans (1954) aggregation index, R' (Eq. (1)), structural complexity index, V (Eq. (2)), mean spatial species mingling, \bar{M} (Eq. (3)), species profile index, A' (Eq. (4)), mean stem-diameter differentiation, \bar{T} (Eq. (5)), Gini coefficient, G' (Eq. (7)), and mean height-diameter ratio of dominant trees, \bar{s} (Eq. (8)). The index values were transformed and standardised so that values indicating low diversity are near 0 and those implying high diversity are near 1.

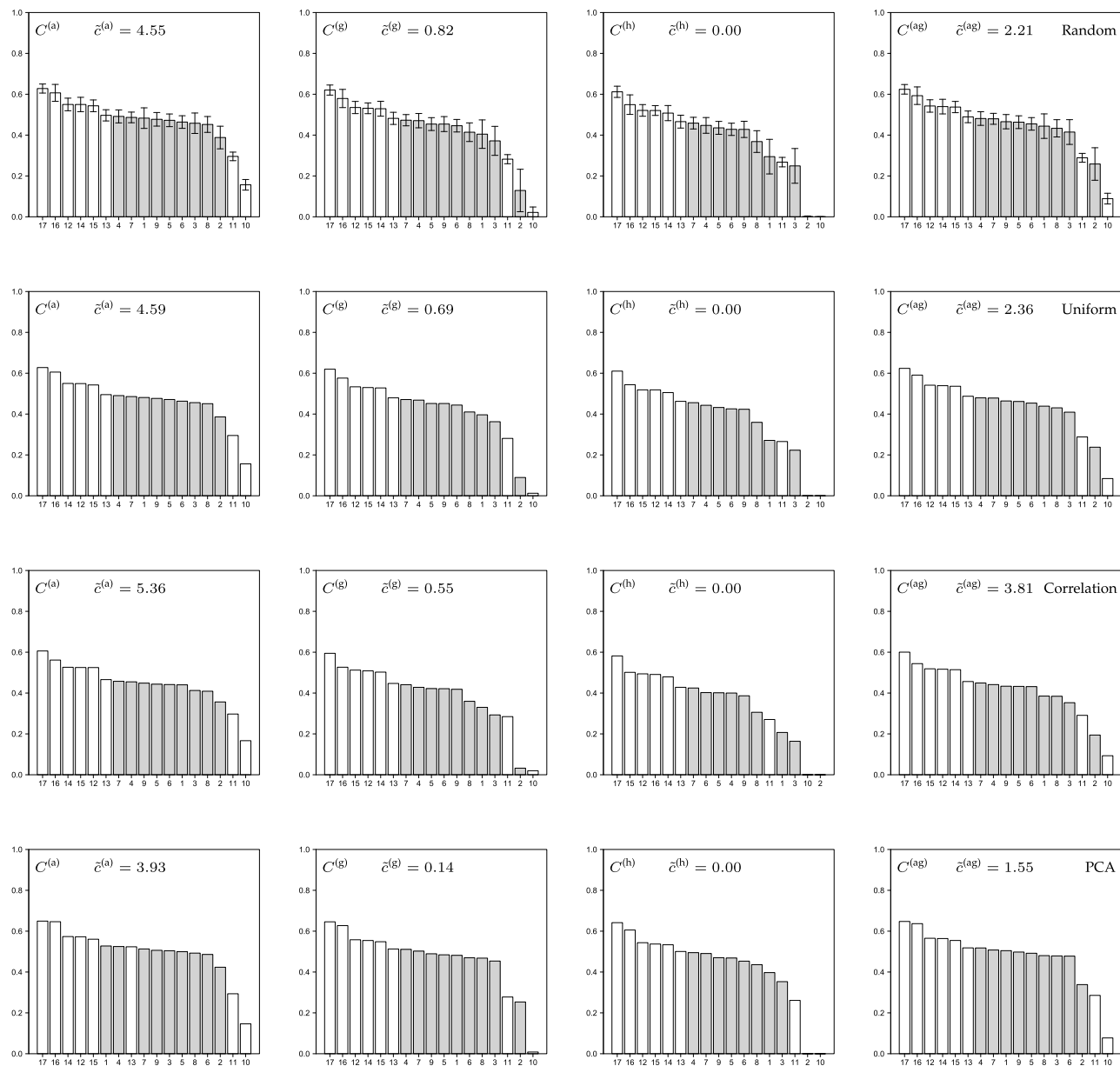


Fig. 4. Bar charts of complexity index C ordered according to complexity and resulting from different weighting methods (from top to bottom: random, uniform, inverse correlation and PCA) and different aggregation methods: $C^{(a)}$ – arithmetic mean (Eq. (9)), $C^{(g)}$ – geometric mean (Eq. (10)), $C^{(h)}$ – harmonic mean (Eq. (11)) and $C^{(ag)}$ – arithmetic mean of arithmetic and harmonic mean. The bars shaded in grey indicate the nine Svarberget plots. \tilde{c} is a linear gradient measure (cf. Section 2.3.3) and the upper index symbols have the same meaning as for C . The numbers on the abscissa give the number of the plots in the order as presented in Section 2.1. The error bars in the first row showing the results for random weighting give plus-minus standard deviation whilst the bar heights represent the means of 1000 simulations.

irrespective of weighting and aggregation methods. Even the ranks of different plots as derived from the respective C values are similar with only minor differences.

Surprisingly, even the use of random weights leads to plausible results that do not differ much from those of other weights. The use of uniform weights, a reasonable default choice, does not introduce major differences compared to the use of random weights. Slightly larger differences in terms of absolute values of complexity index C and the shapes created by connecting the bar tips occur when inverse correlation and PCA weights are applied. From this we can conclude that particularly the choice of weights does not matter much and that all methods used show a fairly robust behaviour, thus inspiring confidence.

When applying geometric and harmonic means (central two columns

in Fig. 4), the complexity-index bars of the least diverse plots are often near zero. This is due to the lesser compensatory nature of these two aggregation methods where values of contributing indices close to zero cause resulting measure C to be near zero as well. This effect leads to sharp drops in the gradients formed by the bars towards the less diverse plots which is avoided when using arithmetic and arithmetic-geometric aggregation.

As expected, linear gradients are best achieved when using arithmetic aggregation (Fig. 4, left column). This is visually supported and also indicated by linear gradient measure \tilde{c} (Section 2.2.3). For both geometric and harmonic aggregation this measure is generally very low. However, \tilde{c} is reasonably large when applying arithmetic-geometric aggregation, i.e. $C^{(ag)}$ (Fig. 4, right column). This method also has the

advantage that the aggregation is not fully compensatory (as for $C^{(a)}$, left column) and thus, for example, a lack of species diversity cannot be fully compensated for by extraordinary size diversity and vice versa. A maximum of measure \tilde{c} is achieved in the right column of Fig. 4 when applying inverse-correlation weights. In this bar chart, also visually the best linear gradient is obtained without any major drops in the height of bars. Therefore we concluded that inverse-correlation weighting combined with arithmetic-geometric aggregation, i.e. $C^{(ag)}$, is the best choice given our data.

3.3. Random weights as references

It makes sense to examine the differences in C between random and non-random weights in greater detail for a better understanding of the influence of different weights on the aggregated complexity indices (Fig. 5).

Looking at general patterns first, it is clear that the differences in terms of uniform versus random weights are very small, i.e. mainly 1–2 % of the maximum of C on average. This is contrasted by the differences in complexity index C caused by inverse-correlation and PCA weights where the differences are around 5–7 % on average. This is still a moderate effect. Another interesting information in Fig. 5 is contributed by the signs of ΔC : Signs are mostly negative when considering the differences to the application of uniform and inverse-correlation weights compared to random weights whilst the signs are largely positive when using PCA weights. Negative ΔC imply that C using the indicated weights is smaller than corresponding C based on random weights, whilst positive ΔC imply the opposite relationship. The opposite trends

of ΔC based on inverse-correlation weights and ΔC based on PCA is a consequence of the aforementioned opposite strategies of the two types of weights, cf. Section 2.3.2. Another general trend is that there is often an increase in ΔC with decreasing C .

Obviously using uniform weights, although seemingly a reasonable choice, only results in small differences in C (Fig. 5, top). This finding can also be concluded by comparing the bar charts of the first two rows of Fig. 4. Here, for all plots C based on uniform weights is slightly smaller than C for random weights. This difference is again largest for plots with low diversity. The signs of ΔC clearly highlight the different strategies of inverse-correlation and PCA weights: On average inverse correlation leads to complexity indices that are smaller than those obtained from random weights, whilst PCA on average yields C values that are larger than those achieved with random weights. The largest values of ΔC across all bar charts in Fig. 5 result from PCA weights and reach 12 % of maximum C .

The trend of increasing ΔC with decreasing C is most likely related to comparatively high weights assigned to contributing indices with low or high values. Since inverse-correlation and PCA weights may for some of these indices be much larger than the corresponding random weights, exceptionally low or high index values are unproportionally decreased or increased in low diversity plots.

3.4. Implications for the Svartherget plots

When accepting $C^{(ag)}$ as the best solution (cf. Section 3.2), the nine Svartherget plots fall into the lower half of the total index range (Fig. 6), whilst the observed maximum is at $C^{(ag)} = 0.60$ (Tazigou).

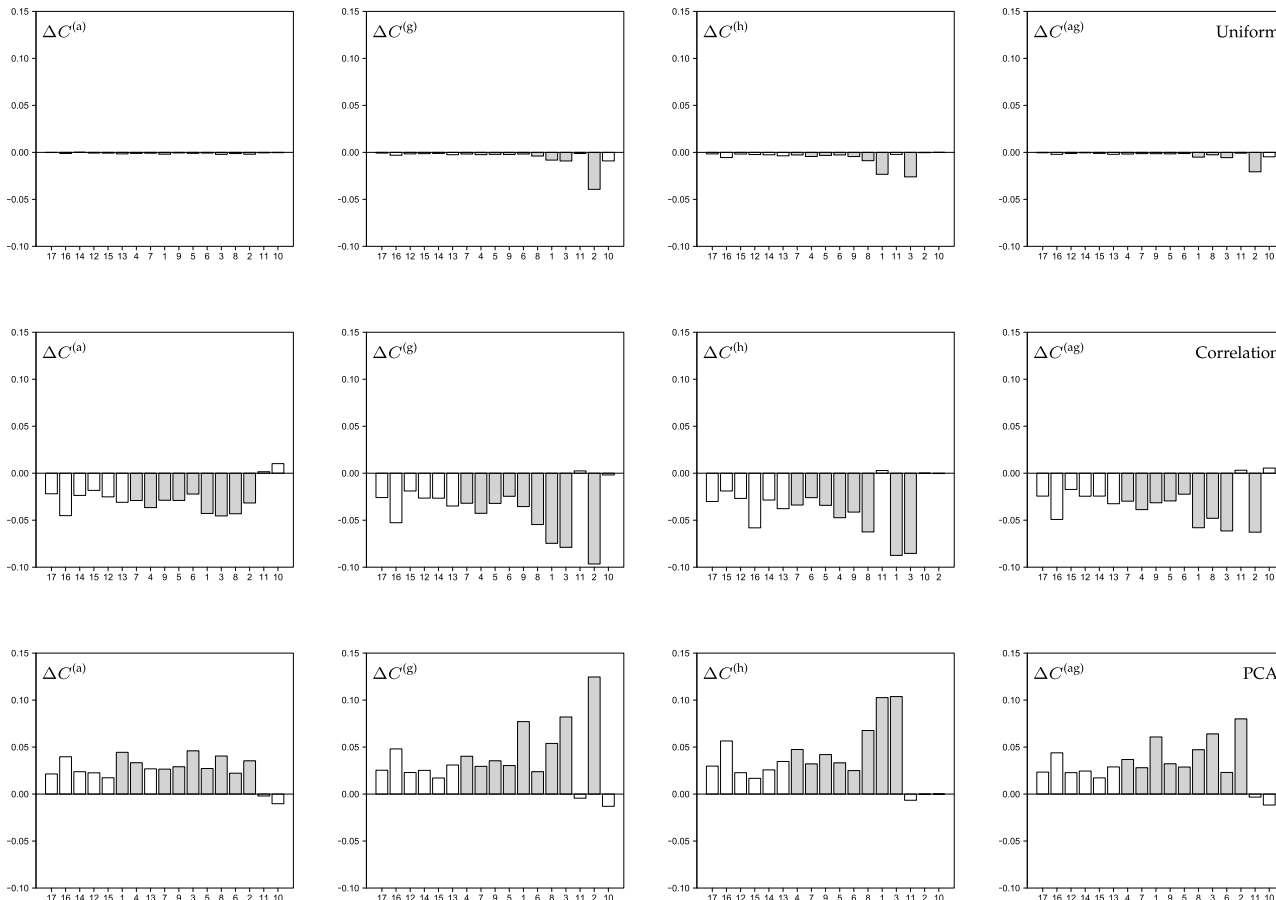


Fig. 5. Bar charts of complexity index difference ΔC , i.e. C ordered according to complexity and resulting from different weighting methods (from top to bottom: uniform, inverse correlation and PCA) minus C ordered in the same way but for random weights. The upper index symbols have the same meaning as in Fig. 4.

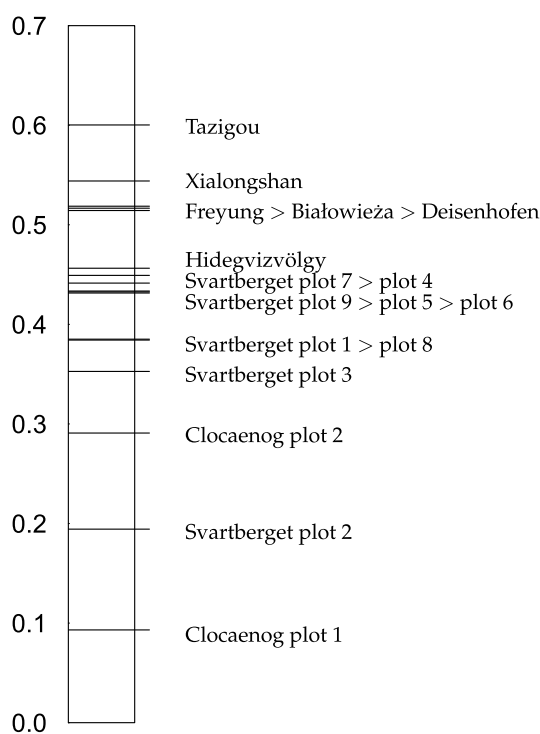


Fig. 6. Complexity index $C^{(ag)}$ values and associated ranks for the nine Svarberget plots and the eight contrast or training plots.

Largely it is only the two Clocaenog *P. sitchensis* plots which are less diverse than the nine Svarberget plots. An exception is Svarberget plot 2 with exceptionally low diversity at $C^{(ag)} = 0.19$ (Table 3) due to comparatively few broadleaved trees. Complexity indices like $C^{(ag)}$ also offer the opportunity to check up on personal perceptions and plot/block selection made ad hoc in the field: We can see that based on means $\bar{C}^{(ag)}$ the blocks allocated to medium and complex structure need to be reversed or at least to be interpreted as similarly complex (Table 3). This is also supported by the lower basal-area density on what is now the medium Svarberget site compared to the complex site (cf. Table 2).

The lower basal-area density is, the more light, nutrients and water are available for the development of complex forest structure. We also understand that the variation of $C^{(ag)}$ is exceptionally high on the simple-structure site, i.e. in plots 1–3. This needs to be taken into consideration when carrying out follow-on analyses.

4. Discussion

We began this article by arguing that diversity is an important notion of ecosystems and even an indicator of resilience and ecosystem health. Many different quantitative measures of diversity have been suggested including non-spatial and spatial measures (Magurran, 2004; Pommerening and Grabarnik, 2019) and measures of functional diversity (Wojcik et al., 2025). Since the statistical methodology commonly used for the aggregation of several such component diversity indices quantified for one ecosystem has to our knowledge not been studied in a systematic way (cf. Ehbrecht et al. 2017, 2021; Wojcik et al., 2025; Zhao et al., 2022), we examined the available approaches in this study (Fig. 2).

Key to the success of the methods applied in this study was a balanced selection of contributing diversity indices from the three α -diversity tenets of location, size and species diversity. Using balanced representations from these three facets of ecosystem structure has also proved useful in spatial reconstruction research, where the structure of forest ecosystems was successfully reconstructed from diversity indicators (Pommerening and Stoyan, 2008; Bäuerle and Nothdurft, 2011; Lilleholt et al., 2014; Wudel et al., 2023). A successful reconstruction of the structure of an ecosystem is only possible, if the characteristics used for the reconstruction are statistically meaningful descriptors (Torquato, 2002). The same is true for an aggregated complexity index. Naturally it is possible to select other indices than those in Section 2.2.1, however, based on our research we are certain that a balanced representation of the three aforementioned tenets is important.

It has proved useful to consider a pool of known and well documented contrast or reference data in addition to the target data. This has not only offered the possibility of plausibility checks by comparing the complexity results and ranks of the target data with those of the reference data but also provided training data for deriving inverse-correlation and PCA weights, which is not too dissimilar to artificial-intelligence applications (cf. Lhoumeau et al., 2025). In contrast to artificial intelligence, while carrying out our analyses it seemed, however, less important to assemble a large, extensive data base of reference plots. More important was the use of reference data with sufficient structural differences so that a meaningful complexity gradient could be established. This gradient made it possible to reliably identify the complexity ranks of the Svarberget plots. If the reference data are sufficiently well diverse, it can be expected that a potential removal or addition of one or two reference data sets or contributing diversity indices has only a minor effect on the complexity indices and ranks of the target plots.

In our study, we considered weight and aggregation method as the most influential parameters of the process of deriving a global complexity index. In our experiments, we applied random, uniform, inverse-correlation and PCA weights. In addition, we used weighted arithmetic, geometric, harmonic and arithmetic-geometric aggregation. Overall the differences in the results between different weights were rather small (Fig. 4). Weights are apparently the weakest of the two influence factors. When comparing weights, inverse-correlation and PCA weights were clearly more influential than random and uniform weights. This is because correlation and PCA weights specifically take the correlation structure into account, whilst the other two weights ignore this statistical structure in the contributing indices.

Our results also revealed that the choice of aggregation is relatively more important than the choice of weights, although both the resulting gradient of global complexity index and the complexity ranks did not differ much even between aggregation methods (Fig. 4). As explained in Section 2.3.3, we were interested in obtaining a complexity gradient as linear as possible aiming at an approximately constant rate of decrease in complexity. This was particularly important for our Svarberget plots, where the structural differences were only small. Linear gradients are best achieved when applying weighted arithmetic aggregation, however, in that case the contributing component diversity indices can fully

Table 3

Complexity index $C^{(ag)}$ for the nine Svarberget plots including arithmetic mean $\bar{C}^{(ag)}$ and coefficient of variation \tilde{v} of $C^{(ag)}$ for the three blocks (simple, medium and complex structure) that were previously selected in the field.

Svarberget plot	Structure type	$C^{(ag)}$	$\bar{C}^{(ag)}$	\tilde{v}
1	simple	0.385		
2		0.194	0.311	0.329
3		0.353		
4	medium	0.441		
5		0.433	0.435	0.013
6		0.431		
7	complex	0.449		
8		0.384	0.422	0.080
9		0.433		

compensate for each other. For example, a lack of species diversity can be compensated for by increased size or vertical forest structure and vice versa. Whilst such compensatory effects make sense and can be justified to some extent, a full compensation seems unrealistic (Thomsen et al., 2024; Hiddink and Davies, 2024). Therefore we identified a hybrid aggregation technique, the weighted arithmetic-geometric method. This method is mostly compensatory but does not allow full compensation. Our results showed that by applying this aggregation method the envisaged linear gradient of complexity indices was developed second best after linear aggregation. A maximum of linearity was achieved with the weighted arithmetic-geometric method in combination with inverse-correlation weights.

The comparison with random weights yielded interesting insights (Fig. 5): Differences between random and non-random weights tended to increase with decreasing overall complexity. Here, contributing indices with particularly low or high values were assigned larger weights than under random conditions. Analysing the differences between random and non-random weights also confirmed the contrasting strategies of inverse-correlation and PCA weights. On average inverse correlation results in complexity indices are smaller than those obtained from random weights, whilst PCA on average yields C values larger than those produced by random weights. To our knowledge using random weights as references has never been attempted before in constructing complexity indices.

The complexity-index values of the Svarberget plots estimated with the weighted arithmetic-geometric method in combination with inverse-correlation weights are plausible when compared with the reference data and field impressions. In comparison with the reference data it is realistic that these boreal forest plots were allocated to the lower half of the complexity range (Fig. 6). However, the results also highlighted that the classification of medium- and complex-structure sites need to be swapped. This is valuable information for future studies involving the Svarberget plots. A maximum $C^{(ag)}$ of 0.60 could be ascertained in our study highlighting that for very large $C^{(ag)}$ near 1 many if not all contributing indices would need to approach their maxima.

Our research has provided greater clarity with regard to the methodology of aggregating individual measures of diversity which is an important precondition for judging on overall biodiversity and for comparing structural complexity with other ecosystem goods and services. Most prominently such comparisons may involve timber and non-timber forest products as economic goods in traditional forestry discourses (Díaz-Yáñez et al., 2019). In addition, the overall complexity index is strongly supported by a number of well-documented individual indices, quantifies structural complexity and allows ranking ecosystems. Structural complexity indices like $C^{(ag)}$ are also likely to play an important role in the transformation of plantations to continuous cover forestry (CCF) and in forest restoration, as increasing structural complexity is an important indicator of successful transformation (Pommerening, 2023).

5. Conclusions

Global structural complexity indices can be successfully derived by aggregating multiple contributing diversity indices. When doing this we found it is useful to analyse research plot data in the context of a small number of reference data that provide sufficient contrast to build a global structural gradient. In our study, inverse-correlation weights combined with arithmetic-geometric aggregation turned out to be the best choice for allowing limited compensatory effects. Generally weights have a minor influence on index aggregation, the aggregation technique used is of greater importance. In this analysis, random weights have turned out to be an important tool for a better understanding of how weights and index aggregation work. Our nine forest plots at Svarberget in Northern Sweden featured at the lower end of the complexity scale and differed comparatively little in structural complexity.

Author contributions

SdS: Data collection, code writing, formal analysis, visualisation, writing of original draft. NS: Data collection, data maintenance, writing of original draft. AP: Conceptualisation, methodology, code writing, formal analysis, visualisation, editing of original draft.

Funding

This research was supported by the Swedish government research council for sustainable development (Formas) grant #2023-00994.

Declaration of generative AI and AI-assisted technologies in the writing process

During the preparation of this work the authors did not use any AI or AI-assisted technologies.

CRediT authorship contribution statement

Sebas de Smedt: Writing – review & editing, Writing – original draft, Validation, Formal analysis. **Norul Sobuj:** Writing – review & editing, Writing – original draft, Formal analysis, Data curation. **Arne Pommerening:** Writing – review & editing, Writing – original draft, Visualization, Validation, Supervision, Software, Resources, Project administration, Methodology, Investigation, Funding acquisition, Formal analysis, Data curation, Conceptualization.

Declaration of competing interest

The authors declare that they have no known financial interests or personal relationships that could have influenced the work reported in this paper.

Acknowledgements

We thank Eliška Eliasson, Michal Kibitlewski, Eric Larmanou, Linnea Larsson, Ida Manfredsson, Mateusz Muzolf, Jenny Viklund and Johan Westin at SLU Svarberget Field Station (Vindeln, Northern Sweden) for their extensive support in collecting the field data. Aila Särkkä (Chalmers University of Technology and University of Gothenburg) kindly provided advice on index aggregation.

Data availability

Data will be made available on request.

References

- Bäuerle, H., Nothdurft, A., 2011. Spatial modeling of habitat trees based on line transect sampling and point pattern reconstruction. *Can. J. For. Res.* 41, 715–727.
- Beckschäfer, P., Mundhenk, P., Kleinn, C., Ji, Y., Yu, D.W., Harrison, R.D., 2013. Enhanced structural complexity index: an improved index for describing forest structural complexity. *Open J. For.* 3, 23–29.
- Begon, M., Harper, J.L., Townsend, C.R., 2006. *Ecology: Individuals, Populations and Communities*, 3rd edition. Blackwell Science, Oxford.
- Beliakov, G., James, S., Nimmo, D.G., 2015. Using aggregation functions to model human judgements of species diversity. *Inf. Sci* 306, 21–33.
- Carmona, C.P., De Bello, F., Mason, N.W., Lepš, J., 2016. Traits without borders: integrating functional diversity across scales. *Trends Ecol. Evol.* 31, 382–394.
- Carvalheiro, L.G., Kunin, W.E., Keil, P., Aguirre-Gutiérrez, J., Ellis, W.N., Fox, R., Groom, Q., Hennekens, S., Van Landuyt, W., Maes, D., Van de Meutter, F., Michez, D., Rasmont, P., Ode, B., Potts, S.G., Reemer, M., Roberts, S.P., Schaminée, J., WallisDeVries, M.F., Biesmeijer, J.C., 2013. Species richness declines and biotic homogenisation have slowed down for NW-European pollinators and plants. *Ecol. Lett.* 16, 870–878.
- Chao, Y.-S., Wu, C.-J., 2017. Principal component-based weighted indices and a framework to evaluate indices: results from the medical expenditure panel survey 1996 to 2011. *PLoS One* 12, e0183997.
- Clark, Ph.J., Evans, F.C., 1954. Distance to nearest neighbour as a measure of spatial relationships in populations. *Ecology* 35, 445–453.

Corral-Rivas, J.J., 2006. Models of tree growth and spatial structure for multi-species, uneven-aged forests in Durango (Mexico). PhD thesis. University of Göttingen (Germany).

Cramer, M., Willig, M., 2005. Habitat heterogeneity, species diversity and null models. *Oikos* 108, 209–218.

Diáz-Yáñez, O., Pukkala, T., Packalen, P., Peltola, H., 2019. Multifunctional comparison of different management strategies in boreal forests. *Forestry* 93, 84–95.

Damgaard, C., Weiner, J., 2000. Describing the inequality in plant size or fecundity. *Ecology* 81, 1139–1142.

Danet, A., Giam, X., Olden, J.D., Comte, L., 2024. Past and recent anthropogenic pressures drive rapid changes in riverine fish communities. *Nat. Ecol. Evol.* 8, 442–453.

Delaunay, H., 1934. Le métabolisme de l'ammonium d'après les recherches relatives aux invertébrés. [Ammonia metabolism based on invertebrate research]. *Annu. Rev. Physiol.* 10, 695–724.

Duduman, G., 2011. A forest management planning tool to create highly diverse uneven-aged stands. *Forestry* 84, 301–314.

Ehbrecht, M., Schall, P., Ammer, C., Seidel, D., 2017. Quantifying stand structural complexity and its relationship with forest management, tree species diversity and microclimate. *Agric. Meteorol.* 242, 1–9.

Ehbrecht, M., Seidel, D., Annighöfer, P., Kreft, H., Köhler, M., Zemp, D.C., Puettmann, K., Nilus, R., Babweteera, F., Willim, K., Stiers, M., Soto, D., Boehmer, H.J., Fisichelli, N., Burnett, M., Juday, G., Stephens, S.L., Ammer, C., 2021. Global patterns and climatic controls of forest structural complexity. *Nat. Commun.* 12, 519.

ElMaraghy, H., AlGeddawy, T., Samy, S.N., Espinoza, V., 2014. A model for assessing the layout structural complexity of manufacturing systems. *J. Manuf. Syst.* 33, 51–64.

Falster, D.F., Westoby, M., 2003. Plant height and evolutionary games. *Trends Ecol. Evol.* 18, 337–343.

Füldner, K., 1995. Strukturbeschreibung von Buchen-Edellaubholz-Mischbeständen. [Describing forest structures in mixed beech-ash-maple-sycamore stands.] PhD thesis. University of Göttingen. Cuvillier Verlag, Göttingen.

Gadow, K.v., 1993. Zur Bestandesbeschreibung in der Forsteinrichtung. [New variables for describing stands of trees]. *Forst Holz* 48, 602–606.

Gadow, K.v., 1999. Waldstruktur und Diversität. [Forest structure and diversity]. *Allg. Forst- Jagdztg.* 170, 117–122.

Gini, C., 1912. Variabilità e mutabilità: contributo allo studio delle distribuzioni e delle relazioni statistiche. [Variability and mutability: contribution to the study of distributions and statistical relationships]. Studi economico-giuridici pubblicati per cura della facoltà di Giurisprudenza della R Università di Cagliari. Tipogr. di P. Cappini.

Hiddink, J.G., Davies, T.W., 2024. Resource limitation of compensatory responses in ecosystem processes after biodiversity loss. *J. Appl. Ecol.* 61, 2382–2391.

Jaehne, S., Dohrenbusch, A., 1997. Ein Verfahren zur Beurteilung der Bestandesdiversität. [A method to evaluate forest stand diversity]. *Forstwiss. Cent.* 116, 333–345.

Kimmins, J.P., 2004. Forest Ecology – a Foundation for Sustainable Management, 3rd edition. Pearson Education Prentice Hall, Upper Saddle River.

Legendre, P., Legendre, L., 2012. Numerical ecology. Elsevier, Amsterdam.

Lhoumeau, S., Pinelo, J., Borges, P.A.V., 2025. Artificial intelligence for biodiversity: exploring the potential of recurrent neural networks in forecasting arthropod dynamics based on times series. *Ecol. Indic.* 171, 113119.

Lilleht, A., Sims, A., Pommerening, A., 2014. Spatial forest structure reconstruction as a strategy for mitigating edge-bias in circular monitoring plots. *For. Ecol. Manage.* 316, 47–53.

Lorenz, M.O., 1905. Methods for measuring the concentration of wealth. *Am. Stat. Assoc.* 9, 209–219.

MacArthur, R., Wilson, E., 1967. The Theory of Island Biogeography. Princeton University Press, New York.

Magurran, A.E., 2004. Measuring Biological Diversity. Blackwell Publishing, Oxford.

Matias, M.G., Combe, M., Barbera, C., Mouquet, N., 2013. Ecological strategies shape the insurance potential of biodiversity. *Front. Microbiol.* 3, 432.

Mazzotti, M., Pareto, A., 2013. Methods for constructing composite indices: one for all or all for one? *Riv. Ital. Econ. Demogr. Stat.* 57, 67–80.

Messier, C., Puettmann, K.J., Coates, K.D. (Eds.), 2013. Managing Forests as Complex Adaptive Systems. Building resilience to the Challenge of Global Change. Routledge, New York.

McElwee, P., 2021. Climate change and biodiversity loss: two sides of the same coin. *Curr. Hist. November* 2021, 295–300.

Moen, R., Gutierrez, R., 1997. California spotted owl habitat selection in the central Sierra Nevada. *J. Wildl. Manage.* 61, 1281–1287.

Oliver, T.H., Isaac, N.J.B., August, T.A., Woodcock, B.A., Roy, D.B., Bullock, J.M., 2015. Declining resilience of ecosystem functions under biodiversity loss. *Nat. Commun.* 6, 10122.

Pommerening, A., Biber, P., Stoyan, D., Pretzsch, H., 2000. Neue Methoden zur Analyse und Charakterisierung von Bestandesstrukturen. [New methods for the analysis and characterisation of forest stand structures]. *Forstwiss. Cent.* 119, 62–78.

Pommerening, A., 2002. Approaches to quantifying forest structures. *Forestry* 75, 305–324.

Pommerening, A., Stoyan, D., 2006. Edge-correction needs in estimating indices of spatial forest structure. *Can. J. For. Res.* 36, 1723–1739.

Pommerening, A., Stoyan, D., 2008. Reconstructing spatial tree point patterns from nearest neighbour summary statistics measured in small subwindows. *Can. J. For. Res.* 38, 1110–1122.

Pommerening, A., Brzeziecki, B., Binkley, D., 2016. Are long-term changes in plant species composition related to asymmetric growth dominance in the pristine Białowieża Forest? *Basic Appl. Ecol.* 17, 408–417.

Pommerening, A., Uriá-Diez, J., 2017. Do large forest trees tend towards high species mingling? *Ecol. Inf.* 42, 139–147.

Pommerening, A., Grabarnik, P., 2019. Individual-based Methods in Forest Ecology and Management. Springer Nature, Cham.

Wang, H., Zhang, X., Hu, Y., Pommerening, A., 2021a. Spatial patterns of correlation between conspecific species and size diversity in forest ecosystems. *Ecol. Modell.* 457, 109678.

Pommerening, A., 2023. Continuous Cover Forestry. Theories, Concepts and Implementation. John Wiley & Sons, Chichester.

Pommerening, A., Sterba, H., Eskelson, B.N.I., 2024. Distance and T-square sampling for spatial measures of tree diversity. *Ecol. Indic.* 163, 111995.

Pommerening, A., Särkkä, A., 2025. Towards a generalization of the spatial species mingling diversity index. *Ecol. Indic.* In review.

Pretzsch, H., 1995. Zum Einfluss des Baumverteilungsmusters auf den Bestandeszuwachs. [On the effect of the spatial distribution of trees on the stand growth]. *Allgemeine Forst- Jagdztg.* 166, 190–201.

Pretzsch, H., 2009. Forest Dynamics, Growth and Yield. From Measurement to Model. Springer, Heidelberg.

Puttkamer, B.v., 2005. A quantitative description of spatial diversity of two zones in the Hidegvízvölgy forest reserve in Hungary. Master thesis. Bangor University, Bangor.

Recher, H., Majer, J., Ganesh, S., 1996. Eucalypts, arthropods and birds: on the relation between foliar nutrients and species richness. *For. Ecol. Manage.* 85, 177–195.

Román-Palacios, C., Wiens, J.J., 2020. Recent responses to climate change reveal the drivers of species extinction and survival. *Proc. Natl. Acad. Sci. U.S.A.* 117, 4211–4217.

Sandifer, P.A., Sutton-Grier, A.E., Ward, B.P., 2015. Exploring connections among nature, biodiversity, ecosystem services, and human health and well-being: opportunities to enhance health and biodiversity conservation. *Ecosyst. Serv.* 12, 1–15.

Simpson, E.H., 1949. Measurement of diversity. *Nature* 163, 688.

Ulrich, W., Bátányi, P., Baudry, J., Beaumelle, L., Bucher, R., Čerevková, A., de la Riva, E., G., Felipe-Lucia, M.R., Galle, R., Kesse-Guyot, E., Rembialkowska, E., Rusch, A., Stanley, D., Birkhofer, K., 2023. From biodiversity to health: Quantifying the impact of diverse ecosystems on human well-being. *People Nat.* 5, 69–83.

Thomsen, M.S., Godbold, J.A., Garcia, C., Bolam, S.G., Parker, R., Solan, M., 2024. Compensatory responses can alter the form of biodiversity – function relation curve. *Proc. R. Soc. B* 286, 20190287.

Torquato, S., 2002. Random Heterogeneous Materials. Microstructure and Macroscopic Properties. Springer Verlag, New York.

Wang, H., Zhang, X., Hu, Y., Pommerening, A., 2021b. Spatial patterns of correlation between conspecific species and size diversity in forest ecosystems. *Ecol. Modell.* 457, 109678.

Weiner, J., Solbrig, O.T., 1984. The meaning and measurement of size hierarchies in plant populations. *Oecologia* 61, 334–336.

Wenk, G., Antanaitis, V., Šmelko, Š., 1990. Waldertragslehre. [Forest Growth and Yield Science]. Deutscher Landwirtschaftsverlag, Berlin.

Wojcik, L.A., Gaedke, U., van Velzen, E., Klauschies, T., 2025. Measuring overall functional diversity by aggregating its multiple facets: functional richness, biomass evenness, trait evenness and dispersion. *Methods Ecol. Evol.* 16, 215–227.

Wold, S., Esbensen, S., Geladi, P., 1987. Principal component analysis. *Chemom. Intell. Lab. Syst.* 2, 37–52.

Wudel, C., Schlicht, R., Berger, U., 2023. Multi-trait point pattern reconstruction of plant ecosystems. *Methods Ecol. Evol.* 14, 2668–2679.

Yachi, S., Loreau, M., 1999. Biodiversity and ecosystem productivity in a fluctuating environment: the insurance hypothesis. *Proc. Natl. Acad. Sci. USA* 96, 1463–1468.

Zenner, E., Hibbs, D., 2000. A new method for modelling the heterogeneity of forest structure. *For. Ecol. Manage.* 129, 75–87.

Zhao, Z., Hui, G., Liu, W., Hu, Y., Zhang, G., 2022. A novel method for calculating stand structural diversity based on the relationship of adjacent trees. *Forests* 13, 343.